# Wave Breaking and Ocean Surface Layer Thermal Response

GEORGE MELLOR

*Program in Atmospheric and Oceanic Sciences, Princeton University, Princeton, New Jersey*

ALAN BLUMBERG

*Department of Civil, Environmental and Ocean Engineering, Stevens Institute of Technology, Hoboken, New Jersey*

17 February 2003 and 25 July 2003

ABSTRACT

The effect of breaking waves on ocean surface temperatures and surface boundary layer deepening is investigated. The modification of the Mellor–Yamada turbulence closure model by Craig and Banner and others to include surface wave breaking energetics reduces summertime surface temperatures when the surface layer is relatively shallow. The effect of the Charnock constant in the relevant drag coefficient relation is also studied.

## 1. Introduction

At one time, the so-called Mellor–Yamada (1974, 1982; hereinafter M–Y) turbulence closure model was thought to produce ocean surface boundary layers that were too shallow during summertime warming and consequently surface temperatures were overly warm (Martin 1985). A recent paper by Mellor (2001, hereinafter M01) investigated two relevant aspects of the problem. First, it was found theoretically, and supported by numerical experiment, that one-dimensional models when forced by a realistic wind stress time series would experience an indefinite increase in surface boundary layer kinetic energy, a process that did not occur in three-dimensional models or in observations. A Rayleigh drag term (Pollard 1970) in the momentum equations resulted in bounded kinetic energy but exacerbated the shoaling problem and increased summertime surface temperatures by a couple of degrees. Then M01, citing experimental evidence, found that the problem could be ''fixed'' by allowing the dissipation term in the turbulence kinetic energy equation to be Richardson number dependent and by introducing an appropriate tuning constant (in a model whose constants were otherwise rather robustly related to neutral data).

Craig and Banner (1994, hereinafter CB) used the M–Y model but modeled wave breaking as a surface diffusion boundary condition of the turbulence kinetic energy equation proportional to $u_\tau^3$ where $u_\tau$ is the surface friction velocity. We had previously thought that the constant of proportionality, $\alpha_{CB}$, of about 100 was rather high and that, in any event, the process would not affect boundary layer deepening. Stacey and Pond (1997), comparing wave-modified profiles with data from Knight Inlet in southwestern Canada, showed that the wave breaking model process beneficially removed sharp velocity shear gradients near the surface. Later, Stacey (1999), analyzing the same data, decided that $\alpha_{CB} = 150$ provided the best fit to his data. Terray et al. (2000) similarly modified the M–Y model and favorably compared calculations with measurements of wave enhanced dissipation greater than the well-known dissipation behavior in the law of the wall, near surface region. Burchard (2001) made a fairly complicated alteration to the $k$–$\varepsilon$ model [which now includes Eq. (2) below; however, $l \propto k^{3/2}/\varepsilon$]; he also obtained much-reduced near-surface shear gradients but no layer deepening for a short, 4-day test case.

In this note we find that, contrary to our prior expectation and, understandably, contrary to the finding of Burchard (2001), the CB surface boundary condition does affect deepening and surface temperature to the extent that the modification of the dissipation term as in M01 can probably be discarded.

## 2. The model

The model equations for turbulence kinetic energy, length scale, momentum, salinity, and temperature are

*Corresponding author address:* Dr. George Mellor, Program in Atmospheric and Oceanic Sciences, Princeton University, P.O. Box CN710, Sayre Hall, Princeton, NJ 08544-0710.
E-mail: glm@splash.princeton.edu

the same as Eqs. (10), (11), (12), and (13) in M01. However, the turbulence energy equation is repeated here; thus,

$$\frac{\partial q^2}{\partial t} = \frac{\partial}{\partial z}\left(K_q \frac{\partial q^2}{\partial z}\right) + 2K_M S^2 - 2K_H N^2 - 2\frac{q^3}{B_1 l}, \quad (1)$$

where $q^2/2$ is the turbulence kinetic energy; $z$ and $t$ are the vertical coordinate and time; $S^2 \equiv (\partial U/\partial z)^2 + (\partial V/\partial z)^2$; $N^2 \equiv -g\rho_o^{-1}\partial\tilde{\rho}/\partial z$; $B_1 = 16.6$ is a model constant; $l$ is the so-called master length scale; and mean velocity shear and potential density gradients are contained in $S^2$ and $N^2$, respectively. A derived result of Mellor and Yamada (1974, 1982) and the level-2½ model is that the mixing coefficients for momentum, temperature (or any scalar), and turbulence are

$$(K_M, K_H, K_q) = lq(S_M, S_H, S_q), \quad (2)$$

where $S_M$ and $S_H$ are functions of $(lN/q)^2$ and we generally set $S_q = 0.41S_H$. Near the surface or in neutrally stratified flow, $(S_M, S_H, S_q) = (0.30, 0.49, 0.20)$.

## 3. Wave breaking parameterization

Following CB, boundary conditions for Eq. (1) are that

$$K_q\frac{\partial q^2}{\partial z} = 2\alpha_{CB}u_\tau^3, \qquad z = 0. \quad (3)$$

Heretofore, $\alpha_{CB} = 0$ in the M–Y model (or its equivalent, $q^3 = B_1 lK_M S^2 = B_1 u_\tau^3$ at $z = 0$). Then, Terray et al. (1996, 1997) found from their observations that

$$\alpha_{CB} = 15(c_p/u_*) \exp[-(0.04c_p/u_*)^4], \quad (4)$$

which is a curve fit to their Fig. 8 of the 1996 paper. The parameter, $c_p/u_*$, is the ''wave age'' where $c_p$ is the phase speed of waves at the dominant frequency, $u_*$ is the air side friction velocity, and $u_* = 30u_\tau$, where $u_\tau$ is the water side friction velocity. For mature waves, where $c_p/u_* \cong 30$, one obtains $\alpha_{CB} \cong 57$ from Eq. (4) whereas for younger waves, where, say, $c_p/u_* \cong 10$, one obtains $\alpha_{CB} \cong 146$, thus independently and convincingly bracketing the values of CB and Stacey (1999).

From the aforementioned papers, one finds that the specification of a finite value of $l$ at $z = 0$ is equal in importance to the stipulation of a nonzero $\alpha_{CB}$. From measured wave heights and near-surface dissipation data, Terray et al. (2000), using the M–Y model, find that a best fit of model output to the data produced

$$l = \max(\kappa z_w, l_z), \qquad z_w = 0.85H_s. \quad (5a,b)$$

[Eq. (5a) is perhaps marginally preferable to $l = \kappa z_w + l_z$ in which case Terray et al. find that $z_w = 1.60H_S$. They used the symbol $z_0$ instead of $z_w$ but the former could be construed as the waterside roughness parameter; the two terms are not necessarily equal.] Thus, $z_w$ scales on the significant wave height $H_S$ (equal to 4× the rms wave height). The ''conventional'' empirical length scale $l_z = l_z(z)$ evokes many prescriptions in the literature, but generally $l_z = \kappa z$ for small $z$ where $\kappa \cong 0.41$ is von Kármán's constant.

The specification of $z_w$ is not simple. Donelan (1990) and Smith et al. (1992) suggest $H_S = 2.0(c_p/u_*)^{2.5}z_0$ [but there are many other formulas cited in Toba et al. (2001); in the choice here, we have rounded the constants slightly], where $z_0$ is the airside roughness parameter and $z_0 = \alpha_{CH}u_*^2/g$ is Charnock's relation. According to Donelan (1990), Smith et al. (1992), and Janssen (2001), $\alpha_{CH} \cong 0.45u_*/c_p$. Putting together these formulas with (5b) yields

$$z_w = \beta\frac{u_\tau^2}{g}, \qquad \beta \cong 665\left(\frac{c_p}{u_*}\right)^{1.5}, \quad (6a,b)$$

where we have converted $u_*$ to the waterside friction velocity, $u_\tau$, in (6a): $u_*^2 = (\rho_w/\rho_a)u_\tau^2$. Stacey (1999), citing observation evidence, chose the value $\beta = 2.0 \times 10^5$.

Since they are uncertain, we wish now to determine the sensitivity of model simulations to the ''constants,'' $\alpha_{CB}$ and $\beta$. For this purpose, we have, as in past papers, used the yearlong Ocean Weather Station (OWS) Papa dataset of Martin (1985) since, when the model performs better or worse for these data, we have found that the same holds for other data. The one-dimensional model grid spans 200 m vertically with 40 grid levels, 9 of which are logarithmically distributed near the surface. An 8-inertial-day, Rayleigh damping is included in the momentum equations as in M01 where it is shown that this or something similar (e.g., tacit adjustment of the Asselin filter in leap-frog temporal discretizations) must be employed in one-dimensional models when trying to simulate real data. For $l_z$ we have used the differential length scale model generally associated with the M–Y model (Mellor and Yamada 1982; M01) but an algebraic length scale parameterization should also work well for surface boundary layer problems. Except for the inclusion of nonzero values of $\alpha_{CB}$ and $\beta$ and deletion of the Richardson-number-dependent dissipation parameterization [the last term in Eq. (1); the dissipation term is not altered in this paper] the model and data details are as described in M01. We have, however, reduced the model time step from 20 to 5 min; this reduced the summertime surface temperature by 0.7°C. Further time step reduction to 1 min reduced the temperature by an additional 0.1°C.

In Figs. 1a and 1b, we plot the surface temperatures for the OWS Papa data together with calculations for the case without wave breaking, $\alpha_{CB} = \beta = 0$, and cases in which $\alpha_{CB} = 50$ and 100 and $\beta = 1 \times 10^5$ and $2 \times 10^5$. The cooler summertime temperatures imply deeper surface boundary layers. Note that the calculations are more sensitive to $\beta$ than to $\alpha_{CB}$.

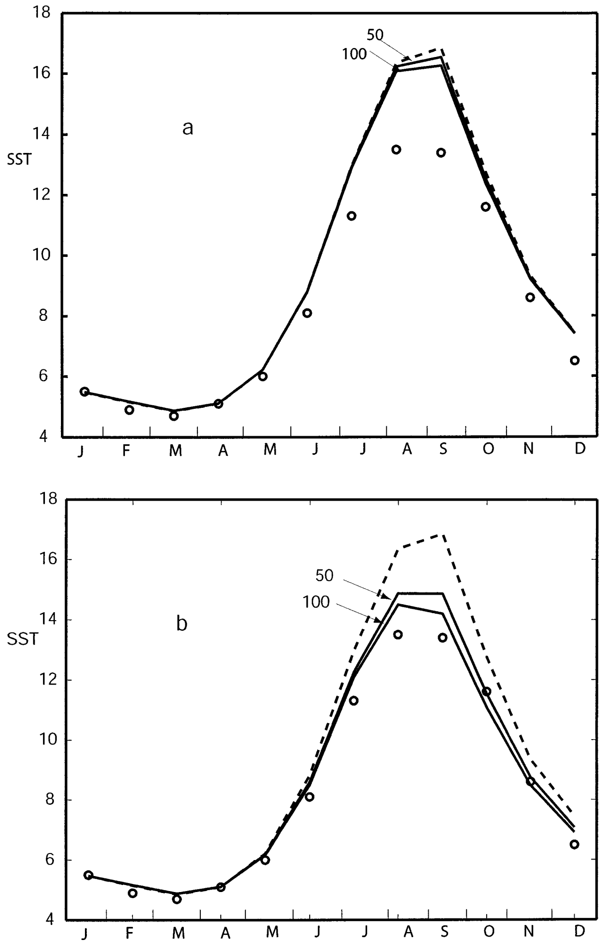


FIG. 1. The circles are the monthly averaged sea surface temperature (SST) measured at OWS Papa for 1961. The solid curves are labeled with values of $\alpha_{CB}$ and (a) $\beta = 1.0 \times 10^5$, (b) $\beta = 2.0 \times 10^5$. The dashed curve is for $\beta = \alpha_{CB} = 0$ in both figures.

## 4. Drag coefficients

While investigating the CB effect on surface boundary layer deepening, we also began to investigate drag coefficients. Martin's well-designed surface forcing code included the familiar equation of Garratt (1977),

$$C_{D10} = (0.75 + 0.067|\mathbf{U}_{10}|) \times 10^{-3}, \tag{7}$$

for the drag coefficient based on wind speed measured at 10 m above the sea surface. Since we borrowed his surface forcing code, we also have been using Eq. (7). Another familiar expression based on the law of the wall is

$$C_{D10} = \left[\frac{\kappa}{\ln(10\ \mathrm{m}/z_0)}\right]^2, \tag{8a}$$

$$z_0 = \max\left(\frac{0.14\nu}{u_*}, \frac{\alpha_{CH} u_*^2}{g}\right), \tag{8b}$$

where $\nu$ is the kinematic viscosity of sea water and $u_*^2 = C_{D10}|\mathbf{U}_{10}|^2$. Figure 2 is a comparison of Eqs. (7) and (8a,b) for $\kappa = 0.41$ and $\alpha_{CH} = 0.0144$, the values of the von Kármán and Charnock constants suggested by Garratt. We have added the smooth wall limit, in the manner of Eq. (8b), which is well established in relatively precise laboratory measurements (Schlicting 1968). The transition from smooth to fully rough is rather abrupt, but Eq. (8b) does produce a drag curve in Fig. 2 that is more in agreement with Eq. (7) than it would be were the smooth and rough terms simply added. As cited above, Donelan (1990), Smith et al. (1992), and recently Janssan (2001; see also Taylor and Yelland 2001) suggest that

$$\alpha_{CH} = 0.45\left(\frac{u_*}{c_p}\right) \tag{9}$$

all from different datasets. Considering a mix of young

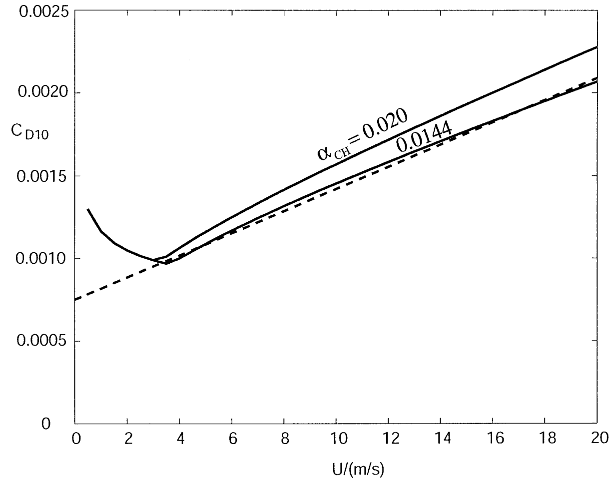


FIG. 2. Drag coefficients as functions of wind speed. The dashed curve is Eq. (7). The solid curves are from Eqs. (8a,b) for the labeled values of $\alpha_{CH}$.

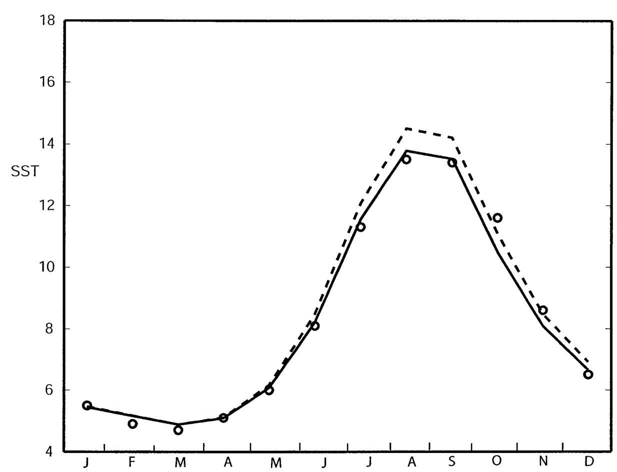


FIG. 3. The dashed curve is the same as in Fig. 1b for $\alpha_{CB} = 100$, where the drag coefficients were obtained from Eq. (7). The solid curve has the same values of $\beta$ and $\alpha_{CB}$ but the drag coefficient uses Eqs. (8a,b) and $\alpha_{CH} = 0.020$.

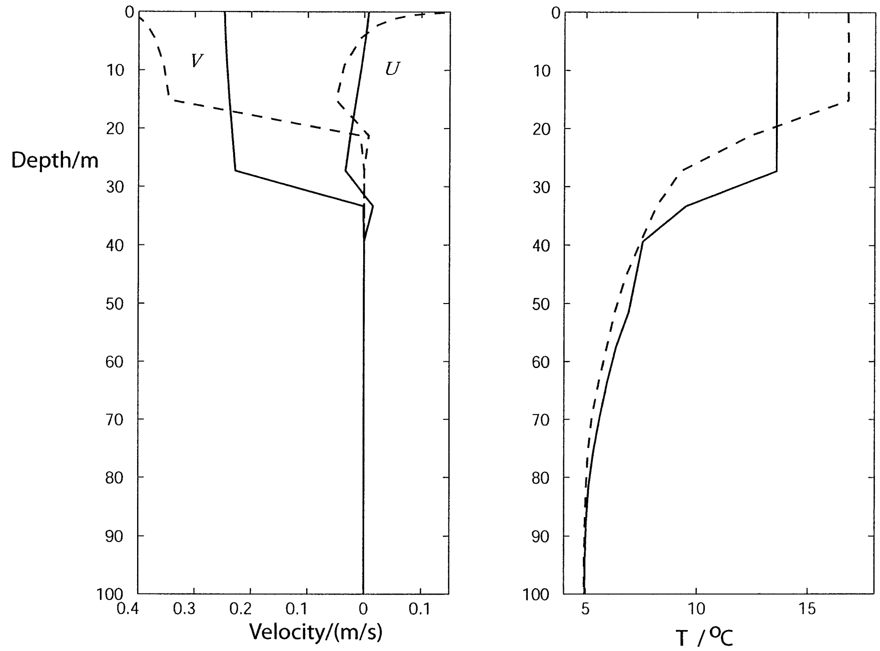


FIG. 4. The velocity component and temperature profiles on 1 Sep, a day on which the surface temperature was close to the warmest temperatures. The dashed lines corresponds to $\alpha_{CB} = \beta = 0$, $\alpha_{CH} = 0.0144$ and the dashed lines in Fig. 1. The solid lines corresponds to $\alpha_{CB} = 100$, $\beta = 2 \times 10^5$, and $\alpha_{CH} = 0.020$, the solid lines in Fig. 3.

waves ($c_p/u_* \cong 10$) and mature waves ($c_p/u_* \cong 30$) would argue for values of $\alpha_{CH}$ larger than 0.0144. Thus, we include drag coefficients for $\alpha_{CH} = 0.020$ in Fig. 2, which yields $C_{D10}$ values about 10% larger than the other curves. It is noted that Donelan et al. (1995) displayed $C_{D10}$ curves that increased by about 50% for young waves relative to mature waves; his values for the mature waves are close to the Garratt values.

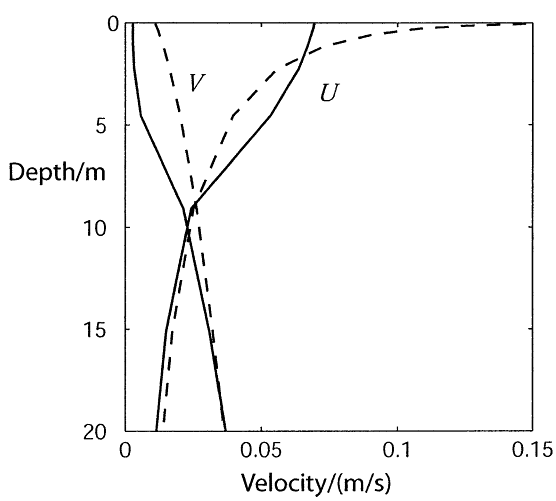


FIG. 5. A detail of the velocity component profiles on 1 May when the wind stress was almost exactly in an east–west direction as is the velocity component, *U*. The layer depth was about 80 m and the nearly uniform temperature of about 5.2°C was unaffected by the Craig–Banner parameterizations. The solid and dashed lines are as described in Fig. 4.

In Fig. 3 we compare calculations for $\beta = 2.0 \times 10^5$, $\alpha_{CB} = 100$ using Eqs. (7) and (8a,b) for $\alpha_{CH} = 0.020$. We note that the rms wind speeds in winter are about 11.5 m s$^{-1}$ and in summer 7.0 m s$^{-1}$; the corresponding average values of $l_0$ are 6.0 and 2.5 m, which seem high if one assumes that Eq. (5b) is correct.

Figures 4a and 4b are plots of the velocity component and temperature profiles on 1 September, a day on which the surface temperature was close to the warmest temperatures. The dashed line corresponds to $\alpha_{CB} = \beta = 0$ and $\alpha_{CH} = 0.0144$, whereas the solid line corresponds to $\alpha_{CB} = 100$, $\beta = 2 \times 10^5$ and $\alpha_{CH} = 0.020$. Figure 4b shows that, as expected, the surface cooling is due to surface boundary layer deepening. This occurs in the summertime when the layer is shallow and therefore affected by surface boundary conditions. In Fig. 4a, one can see that the Craig–Banner parameterizations reduces the surface velocities and this is further emphasized in Fig. 5, which is a detail of the velocity component profiles on 1 May when the wind stress was almost exactly in an east–west direction; the layer depth was about 80 m and the surface temperature was unaffected by the Craig–Banner parameterizations.

## 5. Internal wave parameterization

In Mellor (1989), there was a suggested parameterization to account for the influence of unresolved internal waves in the M–Y model by adding to $S^2$ in Eq. (1) an rms internal wave shear gradient, $\overline{s_{iw}^2} = 0.7N^2$; the constant is based on limited data and is uncertain. Calculations with this parameterization in place yield additional summertime cooling of 0.5°C or less. We have not used this parameterization in this paper, but future insight and data may persuade one to include it. In their modification to the M–Y model, we note that Kantha and Clayson (1994) have assigned considerably more importance to internal wave processes. They include additional (dimensional) diffusivity at the base of the surface boundary layer.

## 6. Summary

The main lesson to be learned is that introducing waves physics into the modeling of surface boundary layers also introduces considerable uncertainty, hardly a surprising conclusion. For users of the M–Y model and maybe other models as well, we tentatively suggest $\beta = 2.0 \times 10^5$ following Stacey (1999), $\alpha_{CB} = 100$, and $\alpha_{CH} = 0.020$. There is little doubt that the first two values should be greater than zero since wave breaking should certainly create a nonzero surface length scale and should provide additional turbulence relative to a flat surface. Furthermore, their orders of magnitude are deemed correct, but more precision will require more data, an interactive wave model and developing confidence in equations like Eqs. (4), (5), and (6). It is seen here that model behavior is apparently more sensitive to the surface length scale than to the amount of turbulence energy injected into the surface.

There is increasing consensus that the Charnock constant should be larger than 0.015, and we believe the value 0.020 is reasonable.

Whereas the need to suppress kinetic energy in one-dimensional models, certainly on climate time scales, is a robust finding in Mellor (2001), this paper may be a good excuse to expunge the Richardson number dissipation parameterization in the same paper lest the model produce too much cooling or until further wisdom is developed. Thus, the basic model is returned to its original form while attention is directed toward wind wave forcing and parameters like wave age.

## 7. Addendum

After the paper was reviewed, we rediscovered an alternate boundary condition for Eq. (3) by CB. In the near-surface region where $l = \kappa z_w$ all terms except the first and last terms in Eq. (1) can be neglected as determined diagnostically from solutions of Eqs. (1), (2), and (3). Then analytical solutions can be found such that $q^3 = q^3(0)\exp(\lambda z)$, where $q^3(0) = (3B_1/S_q)^{1/2}\alpha_{CB}u_\tau^3 = 15.8\alpha_{CB}u_\tau^3$ and $\lambda = [3/(S_qB_1\kappa^2)]^{1/2}z_w^{-1}$. This analytical solution agrees with numerical solutions from Eqs. (1), (2), and (3) near the surface. Also, numerical solutions using Eqs. (1), (2), and

$$q^2(0) = (15.8\alpha_{CB})^{2/3}u_\tau^2 \quad (10)$$

instead of Eq. (3) reproduced all of the calculations in Figs. 1, 3, and 4. The use of Eq. (10) is simpler since it is applied at $z = 0$ whereas, because of the staggered grid that we use, the term $K_q\partial q^2/\partial z$ in Eq. (3) is located at a half grid point below the surface and requires extrapolation to $2\alpha_{CB}u_\tau^3$ at the surface.

*Acknowledgments.* The comments of three reviewers and Dr. Mark Donelan resulted in an improved paper. GLM was funded by the NOPP Surf-Zone Project and by the CBLAST Project, ONR Grant N00014-01-1-0170. Author AB was funded under ONR Grant N00014-03-1-0633.

REFERENCES


Burchard, H., 2001: Simulating the wave-enhanced layer under breaking surface waves with two-equation turbulence models. *J. Phys. Oceanogr.,* **31,** 3133–3145.

Craig, P. D., and M. L. Banner, 1994: Modeling wave-enhanced turbulence in the ocean surface layer. *J. Phys. Oceanogr.,* **24,** 2546–2559.

Donelan, M. A., 1990: Air–sea interaction. *The Sea,* B. LeNehaute and D. M. Hanes, Eds., *Ocean Engineering Science,* Vol. 9, Wiley and Sons, 239–292.

——, F. W. Dobson, S. D. Smith, and R. J. Anderson, 1995: Reply. *J. Phys. Oceanogr.,* **25,** 1908–1909.

Garratt, J. R., 1977: Review of drag coefficients over oceans and continents. *Mon. Wea. Rev.,* **105,** 915–929.

Janssen, P. A. E. M., 2001: Reply. *J. Phys. Oceanogr.,* **31,** 2532–2544.

Kantha, L. H., and C. A. Clayson, 1994: An improved mixed layer model for geophysical applications. *J. Geophys. Res.,* **99,** 25 235–25 266.

Martin, P. J., 1985: Simulation of the mixed layer at OWS November and Papa with several models. *J. Geophys. Res.,* **90,** 581–597.

Mellor, G. L., 1989: Retrospect on oceanic boundary layer modeling and second moment closure. *Parameterization of Small-Scale Processes,* P. Müller and D. Henderson, Eds., University of Hawaii, 251–272.

——, 2001: One-dimensional, ocean surface layer modeling: A problem and a solution. *J. Phys. Oceanogr.,* **31,** 790–809.

——, and T. Yamada, 1974: A hierarchy of turbulence closure models for planetary boundary layers. *J. Atmos. Sci.,* **31,** 1791–1806, Corrigendum, **34**, 1482.

——, and ——, 1982: Development of a turbulence closure model for geophysical fluid problems. *Rev. Geophys. Space Phys.,* **20,** 851–875.

Pollard, R. T., 1970: On the generation of inertial waves in the ocean. *Deep-Sea Res.,* **17,** 795–812.

Schlicting, H., 1968: *Boundary Layer Theory.* 6th ed. McGraw-Hill, 747 pp.

Smith, S. D., and Coauthors, 1992: Sea surface wind stress and drag coefficients: The HEXOS results. *Bound.-Layer Meteor.,* **60,** 109–142.

Stacey, M. W., 1999: Simulations of the wind-forced near-surface circulation in Knight Inlet: A parameterization of the roughness length. *J. Phys. Oceanogr.,* **29,** 1363–1367.

——, and S. Pond, 1997: On the Mellor–Yamada turbulence closure scheme: The surface boundary condition for $q^2$. *J. Phys. Oceanogr.,* **27,** 2081–2086.

Taylor, P. K., and M. J. Yelland, 2001: Comments on ''On the effect of ocean waves on the kinetic energy balance and consequences for the inertial dissipation technique.'' *J. Phys. Oceanogr.,* **31,** 2532–2544.

Terray, E. A., M. A. Donelan, Y. C. Agrawal, W. M. Drennan, K. K.

Kahma, A. J. Williams, P. A. Hwang, and S. A. Kitaigorodski, 1996: Estimates of kinetic energy dissipation under breaking waves. *J. Phys. Oceanogr.,* **26,** 792–807.
——, ——, ——, ——, ——, ——, ——, and ——, 1997: Reply. *J. Phy. Oceanogr.,* **27,** 2308–2309.
——, W. M. Drennan, and M. A. Donelan, 2000: The vertical structure of shear and dissipation in the ocean surface layer. *Proc. Symp. on Air–Sea Interaction,* Sydney, Australia, University of New South Wales, 239–245.
Toba, Y., S. D. Smith, and N. Ebuchi, 2001: Historical drag expressions. *Wind Stress over the Oceans,* I. S. F. Jones and Y. Toba, Eds., Cambridge University Press, 35–53.